LEVITATION FORCE TO TEXTURE CORRELATION IN BULK Y-Ba-Cu-O.

D. CHATEIGNER AND J. RICOTE #
Laboratoire de Physique de l'Etat Condensé, Université Du Maine, Le Mans, France
X. CHAUD
Consortium de Recherche pour l'Emergence des Technologies Avancées, Centre National de la Recherche Scientifique, Grenoble, France
P. GAUTIER-PICARD, E. BEAUGNON and J.-L. SOUBEYROUX
Laboratoire de Cristallographie, Centre National de la Recherche Scientifique, Grenoble, France
C. LEBLOND, I. MONOT
Laboratoire Cristallographie et Sciences des Matériaux, Institut des Sciences de la Matière et du Rayonnement, Caen, France.
present address: Instituto de Cienca de Materiales de Madrid, Consejo Superior de Investigaciones Científicas, Madrid, Spain

Abstract

Neutron diffraction Quantitative Texture Analysis is used to show the correlation between magnetic levitation force and texture in large bulk samples of the Y-Ba-Cu-O high-temperature superconducting systems. Samples are elaborated using the top-seeding process, with or without application of a high magnetic field and thermal gradient. The epitaxial-like texture relationships developed between the two main phases are evidenced, for a fraction of the volume.

Keywords: Correlation texture-levitation, full-pattern QTA, superconductors, $YBa_2Cu_3O_7$

1 Introduction

After twelve years of intensive research, the HTSCs are only barely used technologically, mainly because of the difficulties encountered in the elaboration of these complex systems. This has made the relatively easy-to-synthesise phases $YBa_2Cu_3O_{7-\delta}$ the most studied phase among all others. With critical temperatures around 90 K and relatively high critical magnetic fields, the $YBa_2Cu_3O_{7-\delta}$ (or Y123) phase have interest for its capability to be used as magnetic bearings. Large samples are needed in order to provide large magnetic levitation forces. However, several major facts limit the achievement of large bulks with suitable magnetic properties. First, the main superconducting phase (Y123) is stabilised through peritectic reaction, which causes partial formation of Y_2BaCuO_5 (Y211) influencing the properties, and which needs a precise control of the elaboration cycle. Secondly, the Y123 phase is strongly anisotropic, with critical current densities (Jc) about 10 times larger in the (**a**,**b**) plane than along **c**, which requires the development of strong textures. In levitation devices, the levitation forces are proportional to the product of the field gradient by the magnetisation, which is related to the size of the current loops and to

the Jc of the Y123 phase grains. Since grain boundaries are strongly limiting the current flows through the basal (**a**,**b**) planes (Pernet et al., 1994), large grains oriented with **c** along the magnetisation direction, with a strong alignment of the **a** and **b** axes will prevent grain boundary effects. While many methods have been developed in order to produce strong alignment of Y123 crystallites, neither the effect of texture on levitation, nor the textural relationships between phases, has however been reported in the literature of such systems. We are using here neutron diffraction with position sensitive detector (PSD) and full peak analysis. We then quantitatively describe the textures and correlate them to the levitation forces of Y123 samples.

2 Samples

We have chosen combinations of several techniques for the elaboration of our samples. A $SmBa_2Cu_3O_7$ (Sm123) seed is placed at the centre of the surface pellet prior to melt-texturing (Gautier-Picard et al., 1998). One pellet (Y1) has been processed while applying a 8 T magnetic field (**H**), while the other (Y2) not. Both pellets are processed in the presence of a radial thermal gradient because of the furnace geometry. The after-process diameter is 44 mm and the height 17 mm. The surface is covered by one single grain starting from the seed (Figure 1, left). The growth follows a square pattern imposed by the seed and visible as diagonal growth lines. Three 8x8x8 mm^3 cubes were cut on each pellet and analysed (Figure 1, right): one from the centre (a), one from the edge (b) and a last one from the diagonal (along a seed growth line) near the edge (c). A third pellet (Y3) was prepared without measurable radial thermal gradient nor magnetic field. On this latter we only measured the differences between the centre of the pellet (Y3a) and its diagonal (Y3c). Prior to their characterisation, samples were carefully oxygenated to ensure superconducting properties.

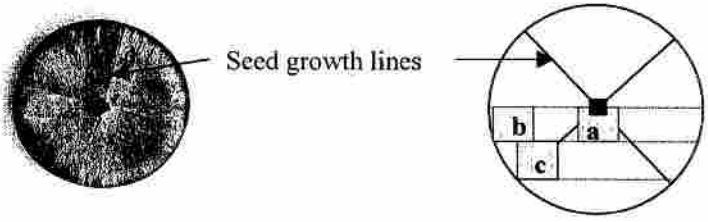

Figure 1: Y2 sample (left) prepared by the top seeded melt-texturing technique without magnetic field, and scheme (right) of the cubic cuts operated on each sample.

3 Experimental

3.1 Levitation measurements

The levitation measurement were performed with a Nd-Fe-B permanent magnet (22 cm diameter, 22 mm high, saturation magnetisation: 0.46 T). The force between the superconductor and the permanent magnet, F, is measured by a strength gage supporting the magnet and is recorded as a function of the distance, z, between the

superconductor and the magnet, using a controlled translation table.

3.2 Texture measurements

Neutron diffraction experiments were carried out at the ILL, Grenoble, using the PSD and the Eulerian cradle of the D1B beam line ($\lambda = 2.523$ Å). We used a 5°x5° grid measurement with 15 s of measuring time for each diagram, and a neutron incidence angle of ω=30°. The Y123 phase crystallises in the Pmmm space group (a=3.81 Å, b=3.88 Å, c=11.66 Å), while Y211 is stabilised in the Pnma space group (a=12.181 Å, b=5.658 Å, c=7.132 Å), parameters that we used for the refinement of the Orientation Distribution (OD). The chosen ω allows to obtain full coverage of the pole figures for $\{112\}_{Y123}$, and blind areas of 10° in the centre of the $\{101/011\}_{Y123}$ and $\{102/012\}_{Y123}$ pole figures. These three pole figures offer enough orientation space coverage to refine the OD of the Y123 phase. We declared the overlaps as the one of the powder.

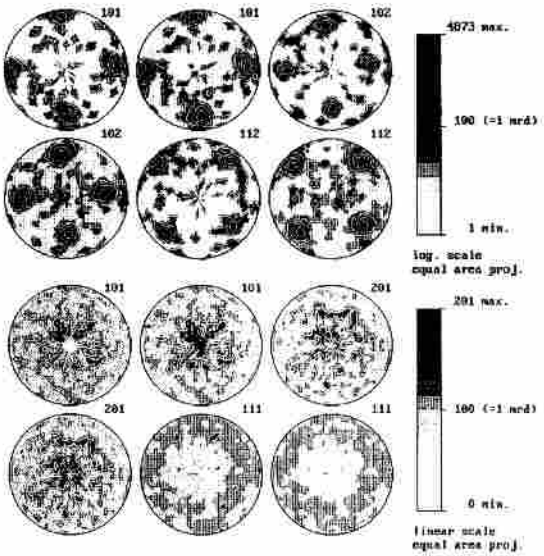

Figure 2: Typical experimental and recalculated pole figures (sample Y1a), to show the reproducibility of the pole figures from the OD refinement for **a):** the major Y123 and **b):** secondary Y211 phases.

For the Y211 phase, we choose the {101}, {201} and {111} non overlapped reflections. The detailed procedure for data reduction and correction is explained in a previous work (Chateigner et al., 1997). The OD was refined with the WIMV algorithm (Matthies & Vinel, 1982) of the Berkeley texture package (Wenk et al., 1998). The RP values for the refinements (Table 1) may appear high for the Y123 phase, but very high texture strengths are obtained (see entropy values and maximum OD). Typical reproductions for these phases are satisfactory as shown on Figure 2 for Y1a. We then recalculated the {001} and {100} pole figures to compare the samples.

4 Results and discussion

4.1 Levitation force

Figure 3 shows the results of the levitation measurements for Y1a, Y1b and Y1c. When the sample is brought to Nd-Fe-B, the levitation force increases up to a maximum value, F(z=0), near the contact. A severe decrease of F is observed with the distance to the centre of the pellet. This decrease is more pronounced for sample Y1 prepared with **H** than for Y2 (not shown here). For the centre of each sample the maximum levitation pressure values, P (Table 1) are comparable. The centre of each sample exhibits the largest P, but interestingly, for the edge, the piece cut along the growth lines exhibits larger P values than the one cut between two lines. For Y1, the edge (b) shows very low P, approximately half of the ones for Y2.

4.2 Quantitative Texture Analysis

Figure 4 shows the recalculated {001} and {100} pole figures of all samples for the major Y123 phase. Textures are very strong as denoted by the very low entropies (Table 1). In general, textures are single (0,0,0) component (Roe/Matthies convention) except Y1b which shows two [(0,0,0) and (280,40,75) in equal proportions]. Looking at samples Y2, with comparable textures (similar OD component and weak random component (FON)), there is a clear correlation between texture entropy and P. P is maximum at the centre where textures reach the strongest values (entropy as low as - 6.6 and OD_{max} = 9500 m.r.d. for Y2a). The lower P(z=0) of Y2b is explained by the larger dispersion of the **c** axes denoted by a OD_{max} value of 1240 m.r.d., the lowest observed for the (0,0,0) single-component samples. When two texture components are present (Y1b), with one tilted from the pellet axis, levitation properties are further decreased. Also, the Y3 samples (Fig. 4, last row), which show the lowest FON, exhibit similar texture strengths to Y2a, and comparable P values.

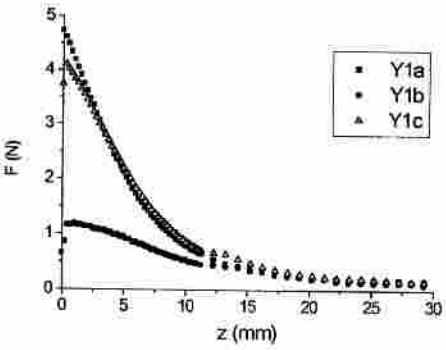

Figure 3: Levitation measurements for Y1 pellet, prepared with a magnetic field.

Comparing Y1 and Y2, we observe a tendency for Y1 to present a larger FON, though weak, than Y2, whatever the location in the pellet (a, b or c). At the same time Y1 shows a lower dispersion of the **c** axes for the (0,0,0) component. These two tendencies play opposite rules regarding entropy and OD_{max} variations. For instance, Y1a with a narrow dispersion of **c** axes and a relatively high FON, presents a larger

entropy and a lower OD_{max} than Y2a. Globally, the Y1 pellet shows a relatively more disrupted texture than Y2 or Y3, may be as a result of a competition between the effect of the applied magnetic forces and grain growth. Without the application of a magnetic field (top seeding only), the texture looks to improve at the global scale, but the component becomes then more dispersed, only guided by the initial seed. With negligible thermal gradient (Y3), the top seed induces comparable texture on the diagonal (Y3c) than at the centre (Y3a).

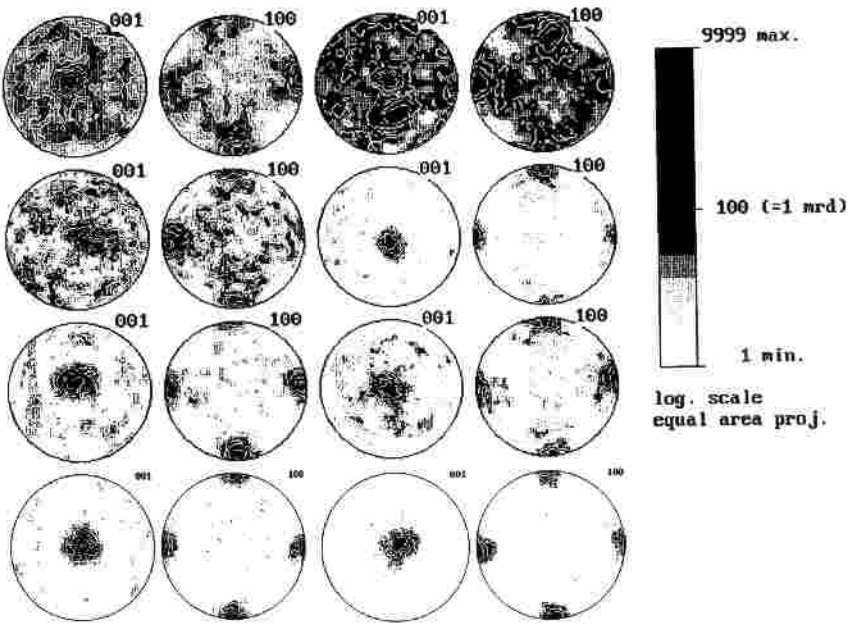

Figure 4: {001} and {100} recalculated pole figures for Y123 in Y1a, Y1b, Y1c, Y2a, Y2b, Y2c, Y3a and Y3c (successive order from top to bottom and left to right).

	P (z=0) (N/cm^2)	Entropy		Max. OD (m.r.d.)		RP0 (%)		RP1 (%)	
		Y123	Y211	Y123	Y211	Y123	Y211	Y123	Y211
Y1a	7.9	-4.97	-0.15	1990	12.0	70	3.36	89	3.39
Y1b	2	-3.20	-0.03	429	3.03	54	2.34	50	2.13
Y1c	6.05	-5.16	-0.14	5370	18.4	61	2.93	71	2.65
Y2a	7.7	-6.57	-0.11	9500	5.67	78	2.56	71	2.17
Y2b	4.4	-4.96	-0.06	1240	8.03	58	1.48	44	1.50
Y2c	5.8	-5.01	-0.04	1520	6.64	51	2.08	38	1.94
Y3a	7.4	-6.36	-0.01	5650	1.62	77	1.84	74	1.35
Y3c	7.9	-6.25	-0.01	6240	1.55	66	2.09	58	1.57

Table 1: Maximum levitation pressure P(z=0) and OD-refinement characteristics for all phases of the samples: entropy and maximum in the OD, RP0 and RP1 reliability factors.

Results for the secondary Y211 phase are presented on Figure 5. This phase is also

oriented, in a much less degree than Y123, with a maximum of the OD around 18 m.r.d. in Y1c. Remarkably, for the samples having the strongest (0,0,0) orientation component for the Y123 phase, the Y211 phase also presents this component. Also, the $\{010\}_{Y211}$ pole figure in these cases shows in-plane orientations corresponding to the $\{110\}_{Y123}$ positions (and the equivalent $\{013\}_{Y123}$ and $\{103\}_{Y123}$ positions by pseudo-symmetry relationships). We believe that this is due to the very similar $\{010\}_{Y211}$ and $\{110\}_{Y123}$ d-spacing which represents a relative mismatch of only 4%.

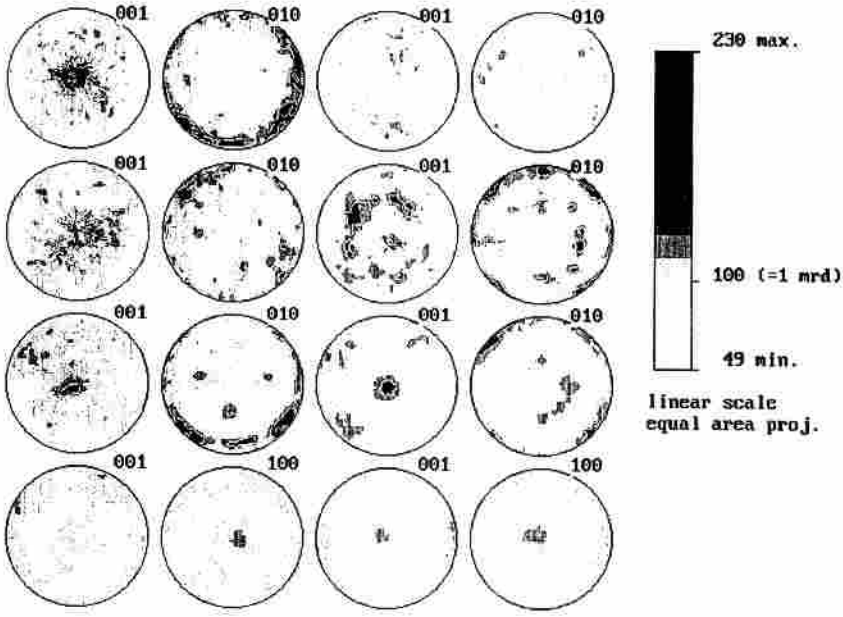

Figure 5: {001} and {010} recalculated pole figures for Y211 in Y1a, Y1b, Y1c, Y2a, Y2b, Y2c, Y3a and Y3c (successive order from top to bottom and left to right).

Without significant thermal gradient (Y3), the Y211 phase is also textured, with a lower strength than in Y1 and Y2, and presents two components, (0,0,0) and (0,90,0), the latter being predominant.

5 References

Chateigner, D., Wenk, H.-R. and Pernet, M. (1997). *J. Appl. Cryst.*, 30, pp 43-48.

Gautier-Picard, P., Chaud, X., Beaugnon, E., Erraud, A. and Tournier. R. (1998), *Mat. Sci. & Eng.*, B53, pp 66-69.

Pernet, M., Chateigner, D., Germi, P., Dubourdieu, C., Thomas, O., Sénateur, J.-P., Chambonnet, D. and Belouet C. (1994). *Physica C*, Vol. 235-240, pp 627-628.

Matthies S. and Vinel G.W. (1982). Phys. Stat. Sol. B 112, K111.

Wenk, H.-R., Matthies, S., Donovan, J. and Chateigner, D. (1998). *J. Appl. Cryst.* 31, pp 262-269.